CHEMICAL FORCE SPECTROSCOPY AND IMAGING

[1]D A Smith, [2]C Robinson, [2]J Kirkham, [3]J Zhang, [1]M L Wallwork
[1] *Department of Physics and Astronomy, University of Leeds, Leeds LS2 9JT, United Kingdom*
e-mail: d.a.m.smith@leeds.ac.uk
[2] *Division of Oral Biology, Leeds Dental Institute, Leeds LS2 9JT, United Kingdom*
[3] *Centre for Nanoscale Science and Technology, Peking University, Beijing 100871, China*

CONTENTS

SUMMARY

The modification of the surface of atomic force microscope probes using ω-functionalised alkyl thiol self-assembly provides a powerful method to probe surface chemical properties with nanometer resolution. Here we review our recent studies of the behaviour of such modified probes under conditions of varying pH, that is, by performing *chemical force titrations*. The chemical force titration behaviour of acid functionalised probes is reviewed and can be adequately described using a model which incorporates two types of hydrogen bonds – a weak, 'normal' hydrogen bond between neutral groups

and a strong ionic bond between neutral and ionised groups. The force titration behaviour of amine self-assembled monolayers (SAMs) is considerably more complex resulting from the higher degree of disorder in amine SAMs of comparable alkyl chain length and also from the competition between amine and thiol groups for gold binding which leads to the presence of both amine and sulphonic acid groups in the monolayer surface. We also review one recent application of chemically modified probes to the mapping of charge on the surface of natural hydroxyapatite, the mineral component of mammalian skeletal tissue, and show that the charge motif that is revealed appears to drive the subsequent binding of proteins on to those surfaces.

I. INTRODUCTION

The strength of intermolecular interactions and their dependence on factors such as temperature, pH and electrolyte concentration have a profound influence on a wide range of chemical and biological processes such as catalysis, protein quaternary structure, enzymatic reactions, protein folding, colloid formation and molecular recognition.

Chemical and biochemical assays have been developed over many years to determine the strength of such interactions. Direct measurement of the interaction between two macroscopic surfaces first became possible when the surface force apparatus was introduced /1/. However, the surface force apparatus only affords very low spatial resolution and it is of great interest in many areas to map surface interactions with molecular or near-molecular resolution. Recently, an instrument has become available that can probe forces at close to molecular spatial resolution and with a force sensitivity that also approaches the molecular level. The atomic force microscope (AFM) /2/ was developed from the pioneering work of Binnig and Rohrer who received the Nobel Prize for Physics in 1986 for their invention of the scanning tunnelling microscope /3/. The AFM has now found very wide application in materials science, physical chemistry, physics and biophysics as a tool that permits imaging of a surface in ambient conditions and under fluids with spatial resolution comparable to electron microscopy, and in some cases with atomic resolution. However, the mode of operation of an AFM, which will be described below, has also provided a tool for measuring and mapping surface and intermolecular forces.

In this review we shall briefly introduce the principles of operation of the AFM as a force sensing instrument and describe methodologies for chemically functionalising the AFM probe so that specific molecular interactions can be measured. Our recent work concerning the effect of ionisation state and ionic strength on the interactions between acid and amine groups will be reviewed. The mapping of charge on skeletal tissue mineral surfaces and the role of the charge domains in driving protein binding will also be reviewed as an example of the application of chemically modified probes for imaging.

2. EXPERIMENTAL METHODS

2.1. Brief Introduction to the AFM

The AFM is one of a family of *scanning probe microscopes* which has grown steadily over the past decade. The AFM uses a flexible cantilever, usually made from silicon or silicon nitride, on the end of which a sharp tip is fabricated using semiconductor processing techniques (see Figure 1). When the tip is brought close to a sample surface the forces between them cause the cantilever to bend and this motion can be detected optically by the deflection of a laser beam which is reflected off the back of the cantilever. If the tip is scanned over a sample surface (using piezoceramic actuators) then the deflection of the cantilever can be recorded as a function of position to produce an image, which in its simplest form, represents the three dimensional shape of the sample surface.

The spatial resolution of AFM depends on many factors but mainly on the sharpness of the tip which can currently be manufactured at best with an end radius of a few nanometers. Atomic resolution AFM images are easily obtained on relatively robust and periodic samples such as graphite or gold. However, soft samples, particularly biological samples, provide a more difficult challenge because the forces exerted by the tip can cause deformation or destruction of the sample. The problems involved with imaging soft samples have been overcome to a large extent by the introduction of tapping mode AFM imaging. Instead of maintaining a constant tip-sample distance of a nanometer or so, the cantilever is oscillated in a direction normal to the sample resulting in only intermittent contact with the surface. This greatly reduces the lateral forces being applied to the sample

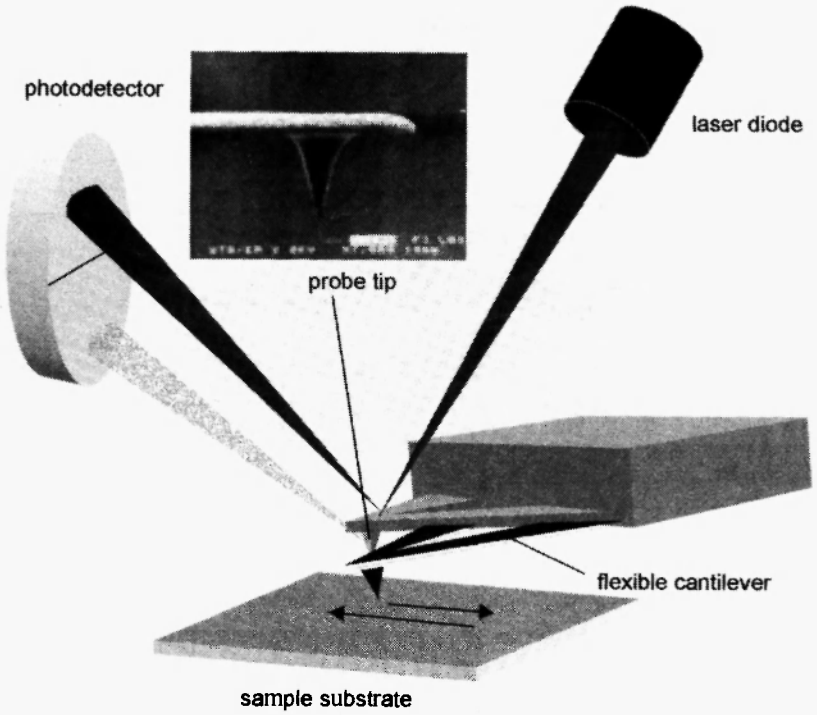

Fig. 1: Schematic drawing of a typical AFM. The microfabricated pyramidal probe tip (SEM side view of an actual tip is shown in the inset) is situated at the end of a light cantilever, the vertical displacement of which is sensed optically by the deflection of a laser beam. The tip is scanned over the sample in a raster fashion (or the sample is scanned under the tip) by piezo-electric ceramics and an image is formed by plotting the cantilever deflection as a function of position over the sample surface.

during scanning that are responsible for most of the damage. The AFM is capable of better than 1 nm lateral resolution on ideal samples and of better than 0.1nm resolution in height measurement.

The significant advantage of AFM as an imaging tool in chemistry and biology when compared with techniques such as electron microscopy is that the sample, which requires no special preparation such as coating, can be imaged under fluids that can be exchanged or modified during the imaging process. The speed of image acquisition is currently limited to the range of

seconds to minutes, which for some processes represents real time. However, in the near future it will be possible to image faster processes on the millisecond time scale due to the development of short cantilevers and other technical improvements.

2.2. Force–distance Measurements with the AFM

The origins of the interaction between tip and sample during imaging can be very complex /1/. Depending on the nature of the sample (and tip) there may be many forces involved including capillary, electrostatic, magnetic, hydrophobic and van der Waal's forces. Consequently, the unequivocal assignment of the origin of the interactions that are observed presents a challenge. Despite these current limitations, the ability of the AFM to probe forces at a surface with high resolution is one of great value and the AFM has found extensive application recently as a force measuring device.

The method that is commonly adopted is to perform what is referred to as a force-distance curve. Here the tip is approached towards the sample, contact is made with a controllable level of applied force and then the tip is retracted from the surface. During this tip approach-retract cycle the deflection of the cantilever is recorded to provide a plot of applied force (when deflection of the cantilever has been converted to force using the cantilever spring constant) versus distance. The form of a simplified force-distance curve is given in figure 2. In part A of the curve the tip is sufficiently far from the surface that no interaction force is experienced until at point B the cantilever contacts the surface. Beyond this point, in section C of the curve, the deflection of the cantilever corresponds to a repulsive applied force (positive in this diagram). In section D, the tip is being retracted and some hysteresis is observed principally due to the characteristics of the piezoactuators. If there is an adhesion between the tip and sample as shown in the example in figure 2 then an attractive force is observed (negative in this diagram) until a critical force (point E) at which the tip suddenly breaks away from the surface (commonly referred to as the pull-off point). In its simplest form, the pull-off point on the force-distance curve provides a direct measurement of the adhesive interaction between the tip and sample.

The interaction between a bare silicon or silicon nitride probe and a surface is likely to be of little interest. However, if the surface chemistry of the tip can be modified in some way then more specific interactions can be probed and in the next section the chemical functionalisation of the tip will be discussed.

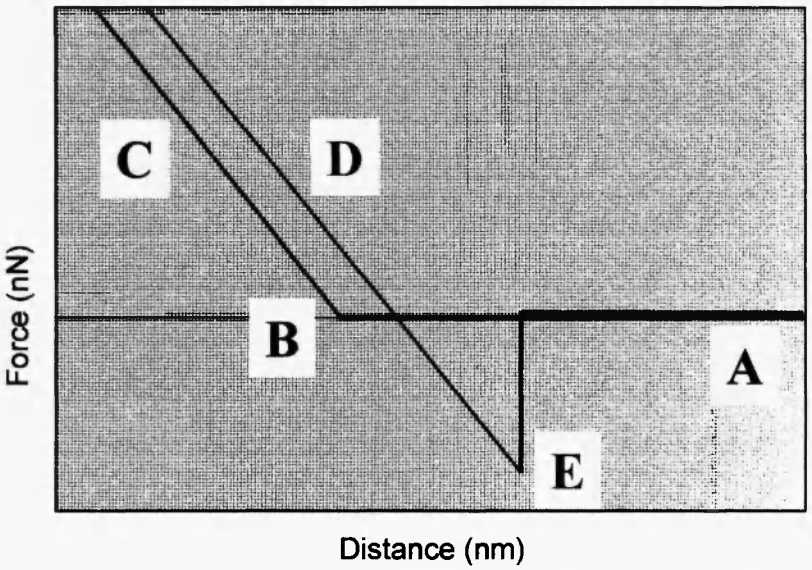

Fig. 2: A typical force distance curve showing the approach (red) and retract (green). A – tip is distant from the surface and no interaction is measured. B - the tip contacts the surface. C – the cantilever is bent and a repulsive force is measured. D – the cantilever holder is retracted from the surface and the measured eventually becomes attractive indicating an adhesive interaction between tip and surface. E – the pull-off point.

2.3. Chemical Functionalisation of AFM tips

Chemical modification of the surface of an AFM probe is most commonly achieved using ω-functionalised alkyl thiols which spontaneously form monolayers (of varying degrees of order depending on a number of parameters) at gold surfaces by formation of a covalent bond between sulphur and gold atoms (see Figure 3). There is an extensive literature on the subject to which the reader is referred for more detailed information about the formation and properties of self-assembled monolayers /4,5/. A range of ω-functionalised alkyl thiols are commercially available including those with methyl, amine, carboxylic acid, hydroxyl and phenyl head groups.

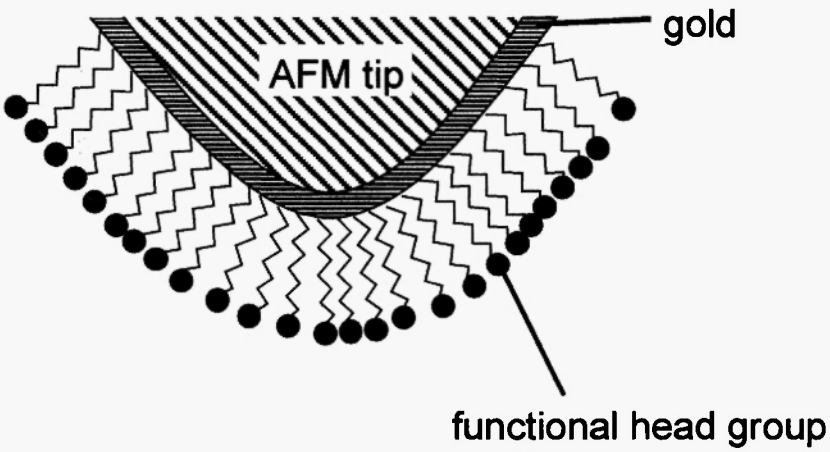

Fig. 3: Modification of a tip with a molecular monolayer by thiol self-assembly. ω-functionalised alkyl thiols are typically used which spontaneously form a monolayer at the surface of a gold film which can be applied by thermal evaporation or sputtering to a tip or glass substrate. The functional group (shown schematically as a solid circle) then provides the new chemical functionality of the tip.

2.4. Chemical Force Titrations

A *chemical force titration* is the name that has been given to the measurement of the adhesion force using chemically modified probes as a function of pH. It is important to note that adhesion titration probes the interaction of the chemically modified tips and substrates *as a function of the* p*H of the bulk solution* not the p*H* at the surface of the molecular monolayers. The p*H* at the surface, pH_s is related to the bulk value, pH_∞, by /6,7/

$$pH_s = pH_\infty + \frac{\psi}{2.303RT/F} \quad , \tag{1}$$

where ψ is the surface potential, R the ideal gas constant, T the absolute temperature and F is the Faraday constant. The pK_a of the surface groups, pK_a^{surf}, is related to the degree of ionisation of the surface, β, and the solution pH_∞ by,

$$\log\frac{\beta}{1-\beta} = pH_{\infty} + \frac{\psi}{2.303RT/F} - pK_a^{surf} \quad . \tag{2}$$

The electrostatic surface potential is not measured by adhesion experiments with the AFM and therefore the quantity $pK_{1/2}$ which is the *solution* pH_{∞} at which half the groups are ionised is often quoted. The electrostatic term arising from the p*H* dependent surface potential is generally of the order 0.1 - 0.5 p*H* units /8/ and therefore the quantity $pK_{1/2}$ is a relatively accurate measure of pK_a^{surf}.

3 CHEMICAL FORCE TITRATIONS WITH FUNCTIONALISED TIPS AND SURFACES

Recently, we have been interested in using chemically modified AFM probes with titratable groups to map the surface charge properties of biological mineral crystals. However, in order to fully understand the behaviour of the modified probes we have studied in detail the interaction between similarly modified tips and flat substrates /9-11/ and it is this work that we review here.

3.1 Experimental

In our work the force-distance curves and adhesion force measurements were performed on a Molecular Imaging picoSPM (Molecular Imaging, USA) controlled by Nanoscope IIIa electronics (Digital Instruments, USA) and Nanoscope software v 4.32. ω-functionalised alkyl thiols were obtained either commercially (16-mercaptohexadecanoic acid, 11-mercaptoundecanoic acid, 3-mercaptopropanoic acid (Aldrich, UK), 11-amino-1-undecanethiol (Dojindo Chemicals, Japan) and 2-aminoethanethiol (Sigma-Aldrich, UK), or synthesised in our collaborators laboratories (11-thioundecyl-1-phosphonic acid) /9/. The mean value of adhesion force was obtained from many hundreds of measurements at different points on the samples.

3.2 Chemical Force Titrations with Acid Functionalised Surfaces

Figure 4 shows the chemical force titration curves acquired at three ionic strengths for tip and substrate both modified with 11-mercaptoundecanoic

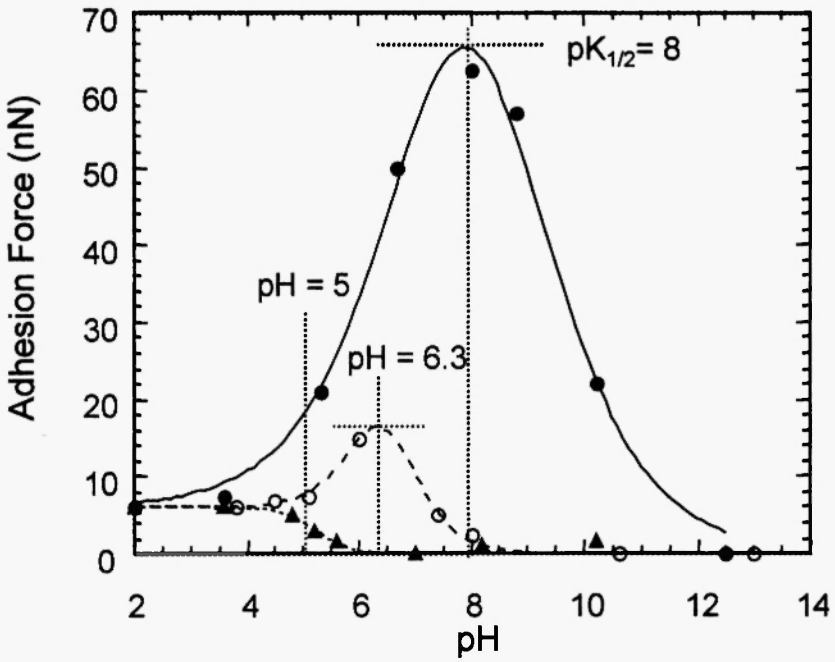

Fig. 4: Chemical force titration curves for tip and substrate both modified with 11-mercapto-undecanoic acid SAMs acquired at three electrolyte concentrations : low electrolyte concentration (~10^{-7} M, solid circles), intermediate electrolyte concentration, (10^{-4} M, open circles) and high electrolyte concentration (10^{-1}M, solid triangles). (The curves have been added only as a guide to the eye).

acid. At very low ionic strength (~10^{-7} M) the force titration takes the form of a single peak of approximately 60 nN centred at pH = 8. At low pH a finite adhesion force of ~6 nN is observed and at pH > 12 almost zero adhesion is measured. At intermediate (10^{-4} M) and high (10^{-1} M) ionic strengths the same adhesion forces are observed at low pH but the transition to zero adhesion occurs at pH values much lower than 12. The force titration peak decreases in size and shifts to lower pH with increasing ionic strength, until at 10^{-1}M, no peak is observed and the force titration curve is sigmoidal with a mid-point at about pH 5.

At low pH values around pH 2, the carboxylic acid groups on tip and substrate will be fully protonated and the finite adhesion force can be

attributed to the formation of complementary hydrogen bonds between the two surfaces. Hydrogen bonding between neutral groups is almost unaffected by ionic strength and an adhesion force of about 6 nN is measured under all ionic strength conditions. At high p*H* values, when the surfaces are fully deprotonated, and the interaction is dominated by the repulsion of two negatively charged surfaces. At intermediate pH the adhesion between the tip and substrate falls off under high ionic strength conditions as the acid groups are deprotonated and the number of hydrogen bonds that form decreases. The sigmoidal shape of the high ionic strength force titration curve can, and has been modelled using the Johnson-Kendall-Roberts (JKR) theory of contact mechanics /1,12,13/ JKR theory predicts this step-like behaviour but not the dramatic deviation to a single large peak at lower electrolyte concentrations.

What is the origin of the peak in the force titration curves of the carboxylic acid SAMs seen under these buffer conditions? There appear to be two possible explanations – either stronger bonds are formed or simply more hydrogen bonds are formed between the tip and substrate.

In order to test these two hypotheses, we measured the chemical force titrations using a diprotic acid, ($PO(OH)_2$) SAM at high and low ionic strength. The reason for our choice of a diprotic acid to test which of the above two hypotheses was correct is as follows. It is well known that acid functionalised SAMs contain a significant degree of in-plane hydrogen bonding with the monolayer /14-16/. It is feasible therefore that when the two SAMs are brought together during the force distance measurements there is some deformation of the two monolayers which disrupts the intra-monolayer hydrogen bonding making more groups available for inter-monolayer bonding and resulting in an increase in the adhesion force. However, in the case of a diprotic acid SAM, one of the ionisable groups lies out of the plane of the monolayer and is therefore freely available for hydrogen bonding irrespective any physical interaction during tip contact. Thus if the same transition from a sigmoidal step to a peak in the force titration is observed for the out-of-plane (lowest pK_a) group it cannot be attributed to a simple increase in the number of hydrogen bonds in this case.

Figure 5 shows the force titration for the phosphonic acid SAM surfaces under high and low ionic strength conditions. Under low ionic strength conditions (10^{-4} M, Figure 5(a)), the force titration curve exhibits two peaks at p*H* 4.6 and 8.4 corresponding to the ionisation of the two hydroxyl groups. When conditions are changed to high ionic strength (10^{-1} M, Figure 5(b)),

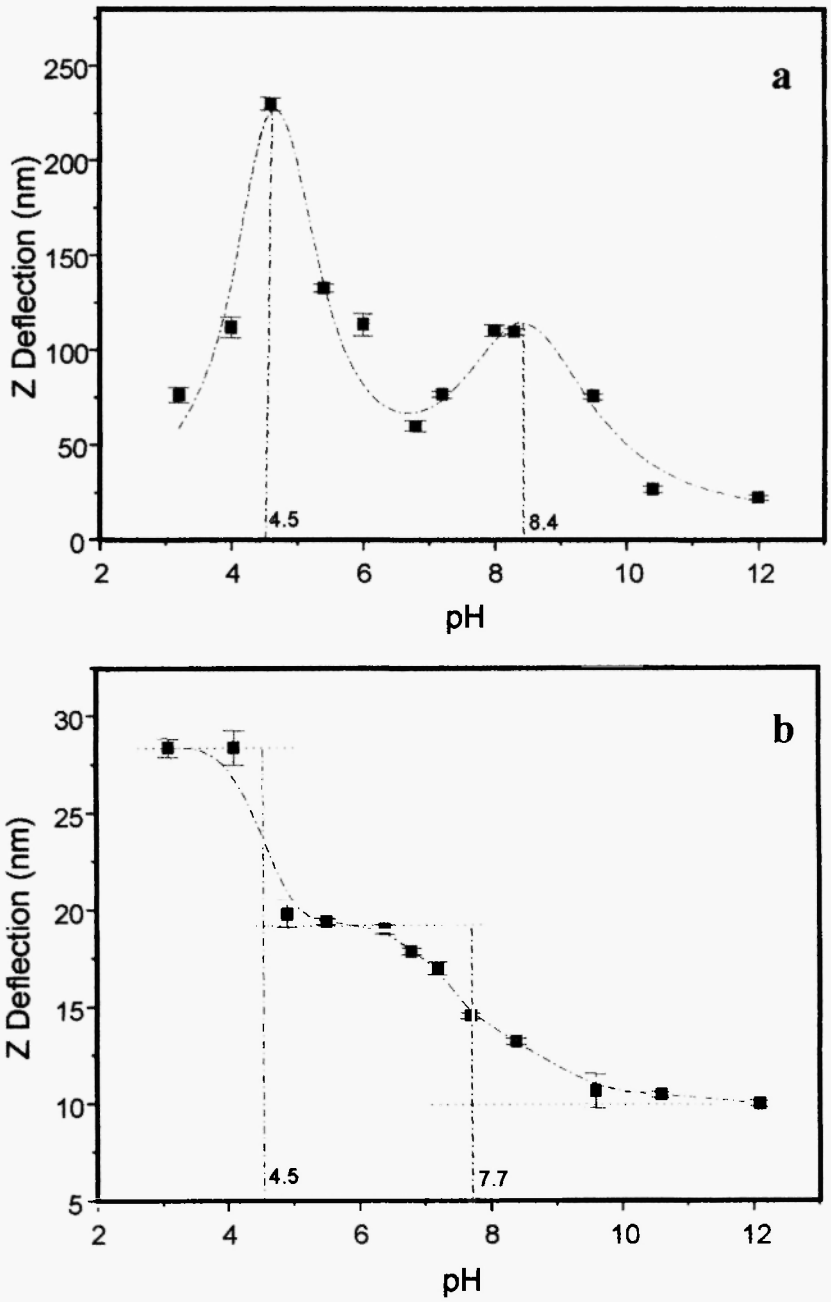

Fig. 5: Force titration curve of 11-thioundecyl-1-phosphonic acid modified tip and substrate in phosphate buffer at ionic strengths a) 10^{-4} M and b) 10^{-1} M.

both peaks are replaced by shoulders with an accompanying shift of the mid-points to lower p*H* (4.6 and 7.7 respectively).

If the peaks in these acid SAM force titrations at low ionic strength are due to the formation of *more* hydrogen bonds, (perhaps permitted by a conformational change in the SAM structure), then we would expect to see a difference between the in-plane and out-of plane groups. However, this is not the case and therefore we must conclude that a *stronger* interaction occurs under low electrolyte concentrations.

What is the origin of the proposed increase in bond strength? Hydrogen bonds formed between ionised and neutral acid groups are predicted to be stronger due to their increased ionic character /17-22/. An extreme example is the HCOOH$\cdots$F hydrogen bond of 60 kcal/mol compared with a normal 'weak' hydrogen bond of a few kcal/mol /23,24/. The anionic HCOOH$\cdots$OOC is predicted, and has been measured in the gas phase, to have a strength of 28-30 kcal/mol /22/. It therefore seems reasonable to assume that the increase in adhesion force that we observe is due to the formation of ionic hydrogen bonds between the two SAMs. However, these short, strong hydrogen bonds exist only under low dielectric constant conditions and small increases in dielectric constant rapidly reduce their strength /18-22/. Under aqueous conditions, one would therefore not expect ionic hydrogen bonds to form, and there has been no experimental evidence to date of ionic hydrogen bonds in systems other than in the gas and crystalline phases. However, it has been shown that solvent is expelled from the interaction volume when the tip and sample are brought into contact /25-28/. The hydration force between a conical tip with a spherical apex and a flat specimen surface at separation distances of the order of 1 water molecule has been calculated to be of the order ~ 0.5 nN /29/. These calculations were performed for a tip of low radii of curvature (~ 4 nm). For tips with a radius of ~ 50 nm as used in these experiments, a hydration force between tip and sample of approximately 4 nN is calculated at a tip sample separation corresponding to the final water layer. The applied force in our experiments is generally higher than this (> 10 nN) and furthermore, tip asperities may lead to a lower applied force before the last water layer is removed /29/. We may therefore assume that the two SAM surfaces come into contact with the displacement of the last remaining water molecule and a concomitant drop in the dielectric constant in the contact area. This is the first example of the direct measurement of ionic hydrogen bonds in a system in an aqueous phase and lends credibility to the hotly debated argument that ionic hydrogen bonds

could be important in biological systems, for example in producing very high enzymatic rates, providing water is expelled from the binding pocket when the substrate binds.

JKR theory has been used to model the high ionic strength force titrations of acid groups and the $pK_{1/2}$ is obtained from the mid-point of the transition /13/. However, clearly the force titration curves are highly dependent on ionic strength and the point at which the $pK_{1/2}$ is measured must therefore be reconsidered. Within the framework of ionic hydrogen bond formation, the $pK_{1/2}$, must lie at the point where the maximum adhesion force is obtained. Above and below the $pK_{1/2}$, the adhesion force decreases because either the number of neutral or ionised groups is falling and each are required to form the stronger bonds. Our low electrolyte concentration data indicate that the $pK_{1/2}$ of the carboxylic acid group is p*H* 8 which is in very good agreement with the pK_a^{surf} values obtained from approach curve data at 10^{-1} M by Hu and Bard /30/ and with the results of Godinez /31/ obtained from cyclic voltammetry at 10^{-1}M.

Why does the size of the adhesion peak fall and its position shift as a function of ionic strength? The reduction in maximum adhesion force with increasing ionic strength is simply due to the interactions of cations from solution with the ionised acid groups in the SAMs and the formation of a complete electric double layer on both surfaces at high enough electrolyte concentration. The effect of changing the ionic strength on the pK_a of groups *in solution* is to shift the value typically by a small fraction of one p*H* unit. However, the $pK_{1/2}$ measured by AFM adhesion appears to be a strong function of electrolyte concentration (the low electrolyte concentration peak is shifted by up to 3 units to higher p*H* in the case of the COOH SAM in comparison with the mid-point of the high electrolyte concentration step). The reason for the shift in the peak can also be accounted for by the association of buffer counterions with the ionised groups in the SAM and the effect this has on the formation of intra- and inter-monolayer $COO^{-}\cdots HO$ bonds. In-plane hydrogen bonding between neutral or neutral and ionised acid groups will tend to stabilise the monolayer and make it more difficult to ionise the remaining neutral groups. At low ionic strength ionic in-plane hydrogen bonding will occur to a high degree and push the $pK_{1/2}$ to higher p*H*. At higher electrolyte concentration these strong in-plane bonds are prevented from forming by the interaction of buffer counterions with the deprotonated acid groups and the remaining neutral groups in the surface are more easily. In addition, the ionic radii of the buffer cations are comparable

to the hydrogen bond length /8,17/ and therefore only a small fraction of the SAM surface need be ionised before the formation of hydrogen bonds between tip and substrate is seriously affected and so the adhesion force drops rapidly to zero at a pH well below the actual pK_a^{surf}, increasing the observed shift between the high and low electrolyte concentration curves.

We have proposed a very simple model based on the formation of strong and weak hydrogen bonds to fit the data. The forces required to rupture one neutral (weak) and one ionic (strong) hydrogen bond may be represented by f_{hb} and mf_{hb} respectively. The total adhesion force due to hydrogen bond formation, F_T, may be easily expressed as a sum of these two interactions,

$$F_T = Nf_{hb}[2(1-\beta)\beta m + (1-\beta)(1-\beta)]. \tag{3}$$

where β is the fraction of ionised groups in the SAM surface and N is the total number of groups within the contact area. Now, the force titration curves are acquired as a function of pH_∞ of the bulk solution not as a function of β, the degree of surface ionisation. The measured p$K_{1/2}$ (which is the *solution* pH_o at which half the groups are ionised), is related to β by,

$$\log \beta/(1-\beta) = pH_\infty - pK_{1/2} \tag{4}$$

and so the total adhesion force may be re-written in terms of the variable α = pH_∞ - p$K_{1/2}$ as,

$$F_T = Nf_{hb}\left[m\frac{2.10^{\alpha}}{(1+10^{\alpha})^2} + \frac{1}{(1+10^{\alpha})^2}\right]. \tag{5}$$

The shape of the force titration curve predicted by this simple model is shown in Figure 6.

Although this model is rather crude, it accurately reproduces the shape of the force titrations and the transition from a peak to a step when the contribution of the strong ionic hydrogen bonds is reduced. However, the peak width in experimental data is not fitted by the model and in the case of the COOH data in Figure 4, the peak is approximately twice the width predicted by the model. We have attributed the increased width of the titration peak to disorder in the SAM surface resulting in heterogeneity in head group environments and therefore a wider distribution of pK_a values than would be expected in a perfectly crystalline, homogeneous monolayer.

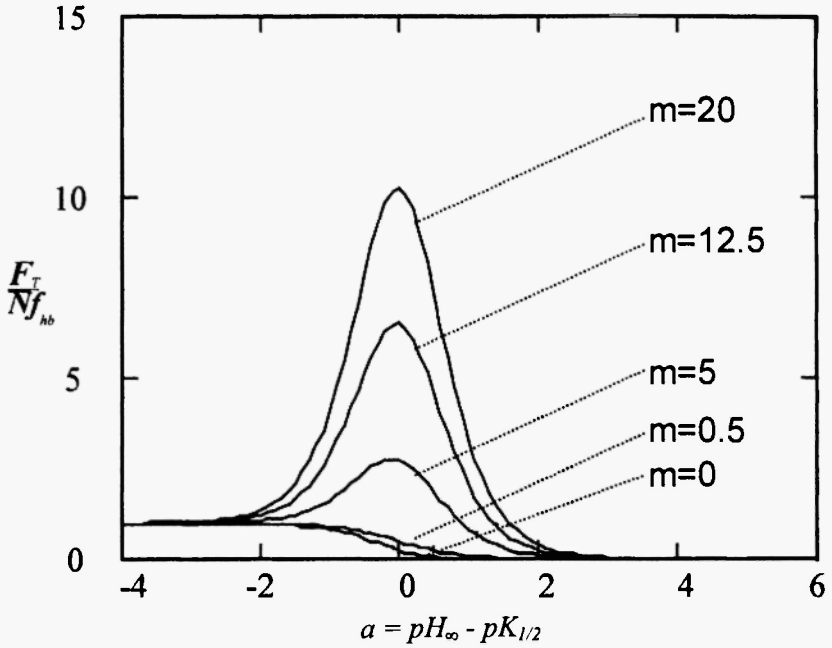

Fig. 6: The total adhesion titration may be modelled as a linear combination of strong ionic and weak neutral hydrogen bonds. The theoretical force titrations produced by this model are plotted for different values of m, the ratio of the strength of these two bonds, and normalised to the product of the number of interacting groups and the strength of a neutral weak hydrogen bond, Nf_{hb}. pH_∞ is the pH of the bulk solution and $pK_{1/2}$ is defined as the pH_∞ at which half the surface groups are ionised (see equation 3). The shape of the low electrolyte concentration curves are reproduced by values of m~15-20, whilst the high electrolyte concentration sigmoidal step is reproduced by m = 0 i.e.no strong hydrogen bonds formed (caused by the interaction of buffer ions with the ionised acid groups in the SAMs (see discussion)).

This hypothesis is easily tested by performing a series of experiments with SAMs of varying alkyl spacer length on tip and substrate since longer alkyl chains are known to produce more ordered monolayers.

Chemical force titrations of COOH SAMs were performed using combinations on tip and substrate of alkyl chains comprising 16, 11 and 3

carbons, namely 16:16, 11:11, 11:3 and 3:3 on tip and sample respectively, and the results are shown in Figure 7. As predicted, the 16:16 carbon spacer SAM force titration is much narrower than the others and the width of this transition is accurately reproduced by our model which has been used to fit the 16:16 data in Figure 7. The slightly lower peak adhesion force that is

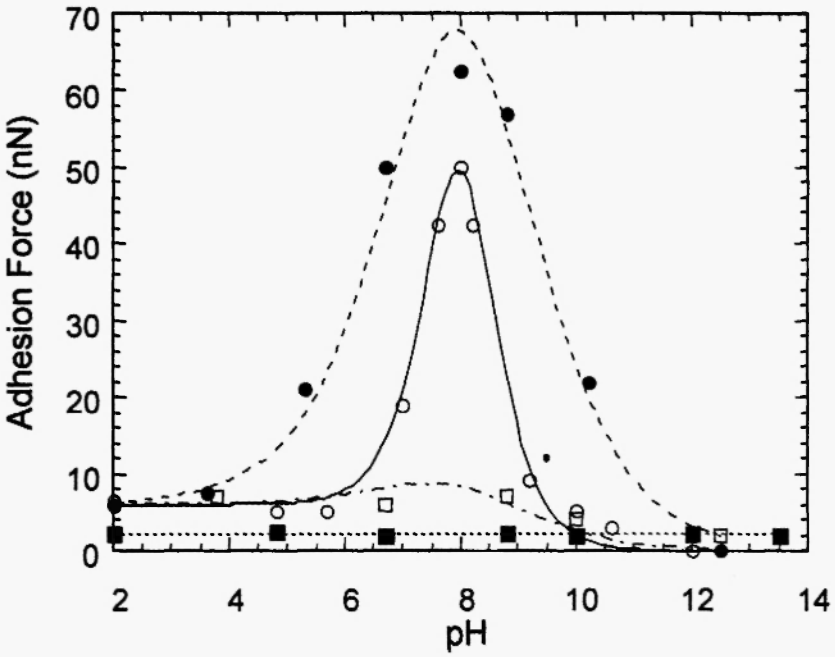

Fig. 7: Chemical force titration curves in very low electrolyte concentration buffer (10^{-7}M) for (a) tip and substrate both modified with 16-mercaptohexadecanoic acid on gold (16:16 open circles), (b) tip and substrate both modified with 11-mercaptoundecanoic acid on gold (11:11 solid circles), (c) tip modified with 11-mercaptoundecanoic acid and substrate modified with 3-mercaptopropanoic acid (11:3 open squares) and (d) tip and substrate both modified with 3-mercaptopropanoic acid (3:3 solid squares). The simple model of figure 6 reproduces the shape of the titration curves but not the width of any but the longest alkyl spacer monolayers due to disorder in the shorter alkyl spacer SAMs. (Curves through the 11:11, 11:3 and 3:3 data are only a guide to the eye, but the 16:16 peak is accurately fitted by the model yielding a value of m of ~16).

measured in the 16:16 system is also probably due to the more highly ordered SAM possessing higher degrees of in-plane hydrogen bonding which compete with the inter-monolayer bonding when the surfaces contact. Using the model to fit 16:16 carbon spacer carboxylic acid force titration data yields a $pK_{1/2}$ of 8 and a value of m of 16, which is in excellent agreement with theoretical predictions and gas phase measurements /17-22/.

3.3 Chemical Force Titrations of Amine Functionalised Surfaces

Figure 8 shows the titration curve for tip and substrate both modified with 11-amino-1-undecanethiol at high and low ionic strength (10^{-1} M and 10^{-4} M respectively). At low pH a small adhesion (< 2 nN) is observed in both high and low ionic strength solutions. At high ionic strength, as the pH is increased the curve follows a sigmoidal step, rising to a maximum adhesion force of 20 nN at ~ pH 5 consistent with previously reported results /13,32,33/. At low ionic strength, the titration exhibits two highly reproducible peaks centred pH 6.2 and pH 9.7 and a very much lower scatter in the data. At pH > 11, the adhesion force decreases in both ionic strength solutions and approaches zero above pH 12. This drop in adhesion force above pH 12 can be reproduced by cycling the pH in the range pH 8-12 and was always observed.

It is the high pH behaviour under both ionic strength conditions, i.e. a drop in adhesion force almost to zero and a second peak or shoulder at low ionic strength, that is difficult to explain within a framework of inter- and intra-monolayer hydrogen bonding. The large adhesion force observed above pH 5 in the high ionic strength force titration is similar in magnitude to the adhesion between methyl terminated SAM surfaces shown independently by Vezenov *et al.* /13/ and van de Vegte *et al.* /33/ and repeated in our laboratory.

In addition, recent force titration work performed on patterned SAMs /34/ comprising COOH and CH_3 regions has shown that the hydrophobic interaction in the CH_3 areas shows a wide scatter in the measured adhesion as we have observed for amine SAMs. It seems reasonable therefore that the scatter and high adhesion force observed for amine SAMs are due to the interaction of two hydrophobic surfaces which arise from the exposure of the alkyl chains in a disordered monolayer.

Why does the adhesion force drop to zero at high pH if it is simply due to hydrophobic forces and what is the origin of the high pH feature in the low

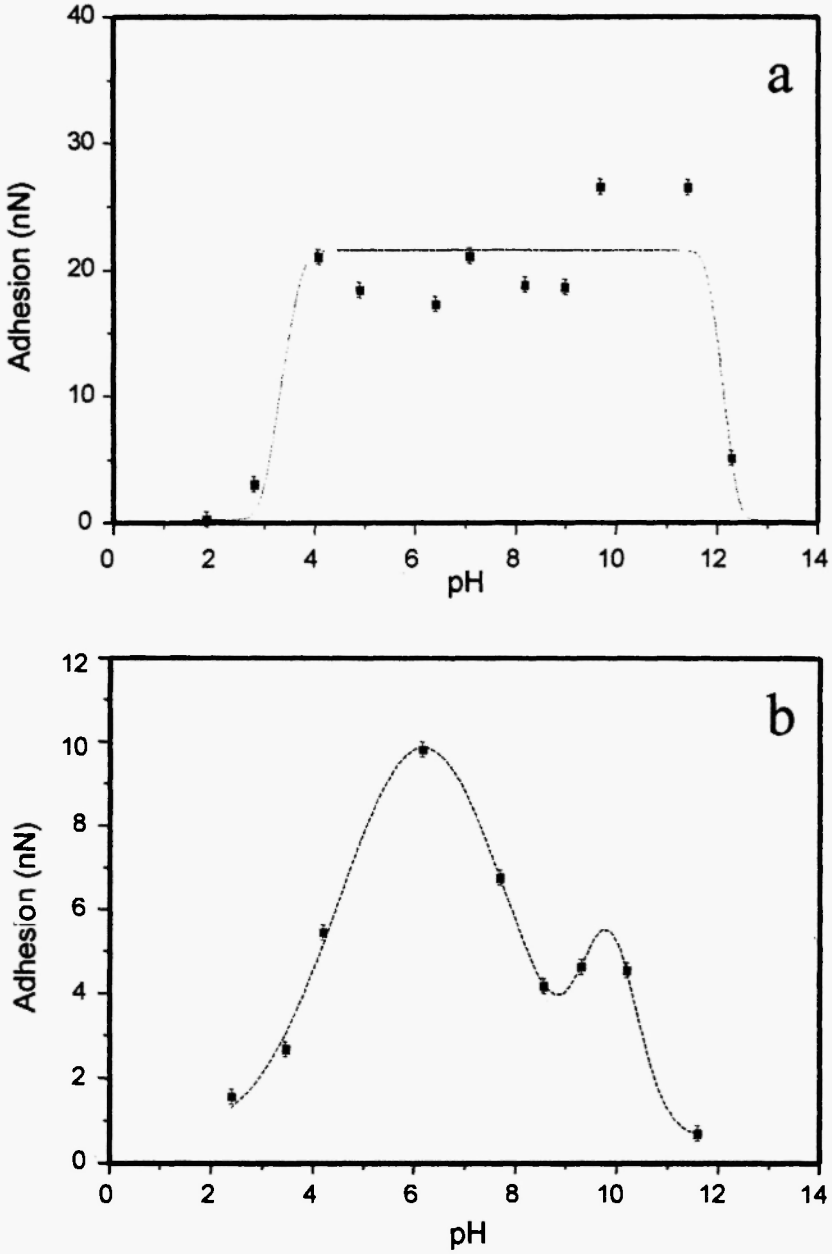

Fig. 8: Chemical force titration curves for tip and substrate both modified with 11-amino-1-undecanethiol SAMs acquired under solutions of two ionic strengths : (a) 10^{-1} M and (b) 10^{-4} M. (The curves have been added as a guide to the eye).

ionic strength curve? It has been postulated that amine groups compete with thiol groups for binding to the gold surface /35-39/ during SAM formation. If this is the case, then this would result in a surface containing both amine and sulphur groups which would probably oxidise under the experimental conditions to form sulphonic acid groups. The drop in adhesion at very high p*H* in our data could therefore be explained by an electrostatic repulsion between two surfaces containing ionised acid groups as well as neutral amines. The presence of charged groups in the SAM at high pH is supported by the long range electrostatic repulsion observed in the approach part of the force-distance curves shown in Figure 9.

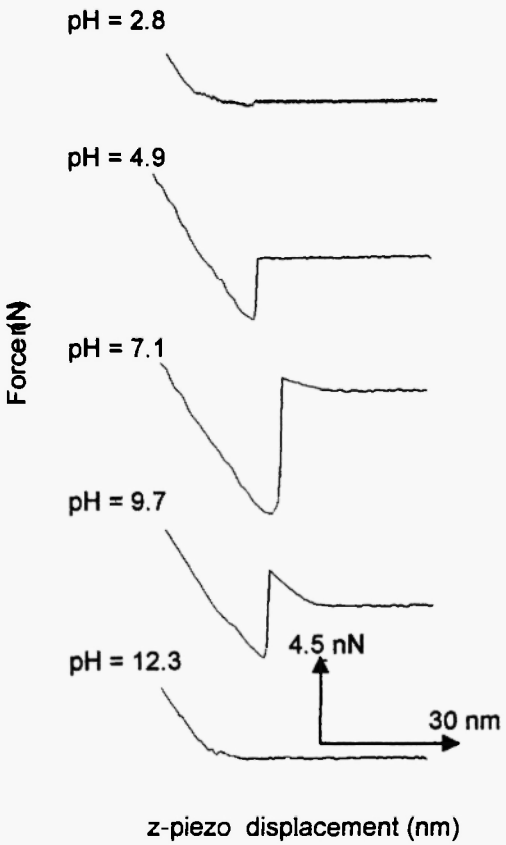

Fig. 9: The approach sections of representative force-displacement curves at different pH values for an 11-amino-1-undecanethiol SAM modified tip and similarly modified substrate in high ionic strength buffer (10^{-1} M).

At very low pH there is an electrostatic repulsion between electric double layers formed on positively charged NH_3^+ surfaces that dominates the approach curve as expected. In the intermediate pH range, the attractive interaction dominates and a jump to contact is observed which disappears at high p*H* (p*H* = 12.3) when the curve is once again dominated by a repulsive force which can only be attributed to ionised groups in the SAM. The presence of an ionisable acid group can also explain the second feature in the force titration curve at high pH by invoking the idea of a stronger ionic hydrogen bonding or even an attractive electrostatic interaction between charged groups on the two surfaces.

As in the case of the acid SAMs, the alkyl chain length has a strong effect on the force titration curve of the amine SAM. Figure 10 shows the chemical force titration curves for combinations of carbon chain length amine SAMs (11 : 11, 11 : 2 and 2 : 2) on tip and substrate respectively. The peak at lower p*H* is attributed to a hydrophobic interaction arising from SAM disorder since it increases in magnitude with a decrease in spacer length. The second peak is almost unaffected in magnitude or position by the carbon spacer length, but as we have seen is strongly affected by ionic strength and therefore must be electrostatic in origin.

The complex behaviour of the amine SAM therefore appears to be due to disorder (which may be tip induced in a more disordered fluid monolayer), which gives rise to a hydrophobic interaction when the two surfaces are brought together and due to the presence of acidic ionisable groups in the monolayer.

4 APPLICATION : MAPPING OF CHARGE ON SKELETAL TISSUE MINERAL SURFACES

The control of skeletal tissue mineral growth and dissolution by proteins is a process of great importance in the understanding and eventual treatment of pathologies such as osteoporosis, ectopic calcification and dental cares. Precise control mechanisms remain obscure but interactions between crystal surfaces and specific stereochemical arrays on extracellular matrix proteins have been implicated /40/.

Dental enamel is the most extreme case of mammalian biomineralisation. During enamel formation, very thin, ribbon-like crystals of hydroxyapatite are initially deposited in a complex extracellular organic matrix, composed

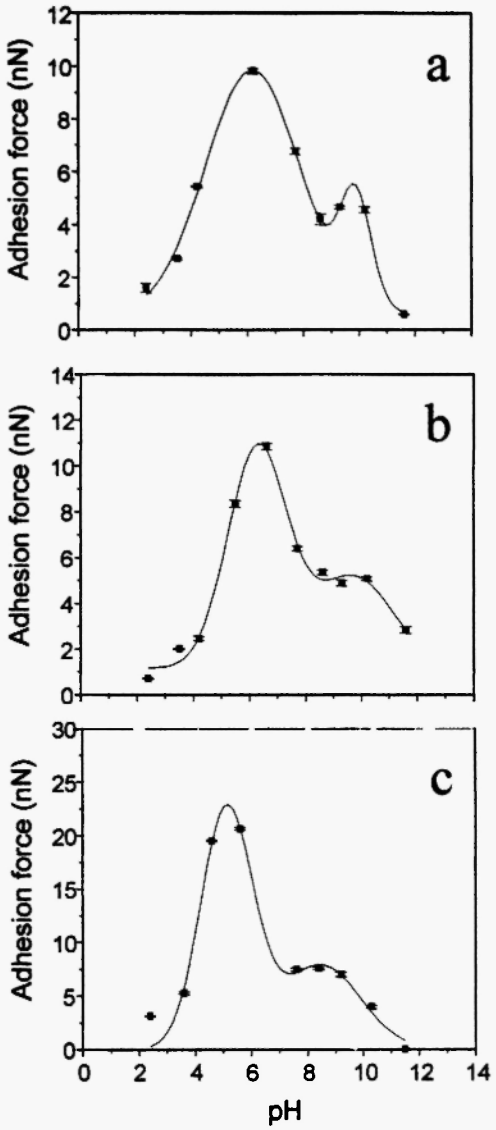

Fig. 10: Chemical force titration curves obtained in low ionic strength (10^{-4} M) buffer for (a) both tip and substrate modified with an 11-amino-1-undecanthiol monolayer (alkyl spacer length 11 carbons), (b) tip modified with an 11-amino-1-undecanethiol monolayer and substrate with a 2-aminoethanethiol (alkyl spacer length 2 carbons on substrate) and (c) both tip and substrate modified with a 2-aminoethanethiol monolayer. (The curves have been added as a guide to the eye).

primarily of a family of related proteins derived from a single gene – the amelogenins /41/. Recently, we have been applying the technique of chemical force microscopy to the surfaces of natural hydroxyapatite using titratable chemical groups in order to map the surface charge distribution of the crystals and to subsequently investigate whether protein binding *in vitro* is driven by these charge motifs.

Chemical force microscopy (CFM) using COOH and NH_2 functionalised tips in their ionised states was used to interrogate the surfaces of individual maturation stage crystals in an attempt to identify variations in surface charge. CFM revealed repeating alternating domains of surface charge in the direction of the crystallographic "c" axis (Figure 11 (a) and (b)), comprising broad bands (30-50 nm in width) interrupted by narrower domains (approx. 15 nm in width). Negatively and positively charged tips produced images which were the inverse of each other indicating that the banding pattern observed was due to distinct differences in charge, or charge density, at the crystal surface. The corresponding height images (Figure 11 (a) showed no evidence of surface features which might induce artefacts in the CFM images

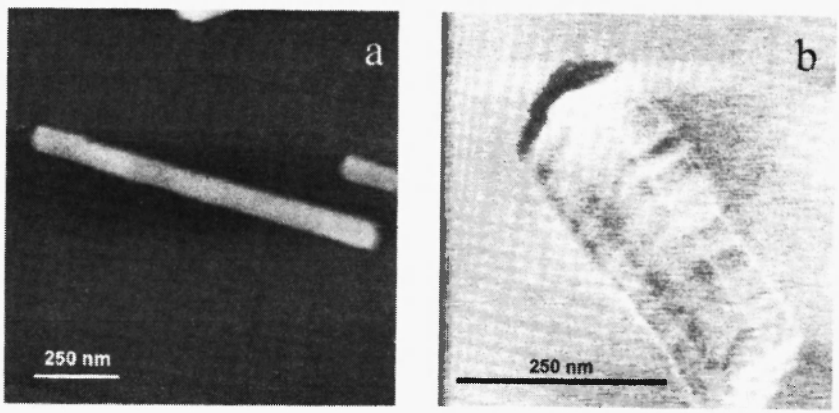

Fig. 11: Surface characteristics of hydroxyapatite crystals isolated from the developing enamel of rat incisor teeth; imaged under fluid at pH 7.4. (a) Typical AFM (height) image of crystal obtained using unmodified tip. Crystal surfaces are typically very smooth. (b) CFM image obtained in lateral force mode using carboxyl-modified tip. Bands of high and low friction, corresponding to alternating charge domains can be seen.

nor have any banding patterns been observed in previous AFM studies with unmodified tips /42-44/.

The role of these charge domains in driving the binding of matrix proteins is graphically illustrated in Figure 12. This figure shows a fluid tapping mode AFM image of a maturation stage enamel crystal after the addition of one of the major constituents of the enamel matrix, M179 amelogenin. The protein is clearly seen to bind in a striped pattern that reflects the underlying charge distribution revealed by chemical force microscopy.

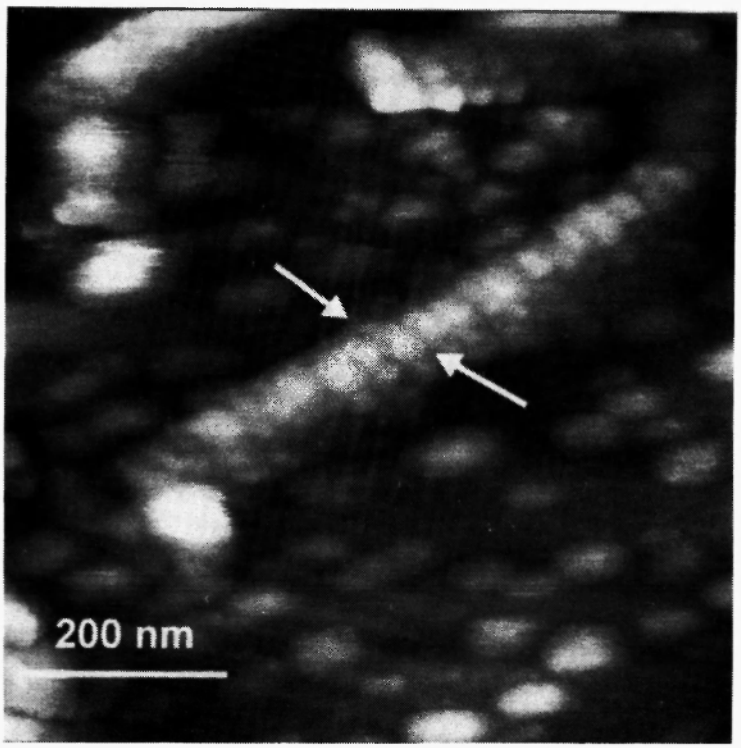

Fig. 12: Tapping mode AFM image in aqueous buffer of a maturation stage enamel crystal after the addition of M179, one of the principal constituents of the organic matrix. The protein can be clearly seen to bind in a banded patter highly reminiscent of the banded charge pattern that was revealed by CFM.

5 CONCLUSIONS

The modification of the surface of AFM probes using ω-functionalised alkyl thiol self-assembly provides a powerful probe of surface chemical information with nanometer resolution. Here we have reviewed our studies of the behaviour of such modified probes under conditions of varying p*H*, that is, by performing *chemical force titrations*, and the application of these probes to one specific example, that of charge mapping of natural skeletal mineral crystals.

The chemical force titration behaviour of acid functionalised probes can be adequately described using a model which incorporates two types of hydrogen bonds – a weak, 'normal' hydrogen bond between neutral groups and a strong bond between neutral and ionised groups. The ionic hydrogen bonds have been measured to be approximately 16 times stronger than neutral hydrogen bonds. The force titration behaviour of amine SAMs is considerably more complex resulting from the higher degree of disorder in amine SAMs of comparable alkyl chain length and also from the competition between amine and thiol groups for gold binding which leads to the presence of both amine and sulphonic acid titratable groups in the monolayer surface.

Chemically modified probes have been successfully applied to the mapping of charge on a biological surface. The surface of interest is that of natural hydroxyapatite, the mineral component of mammalian skeletal tissue. Chemical force microscopy using positive and negatively charged tips was used to map the surface charge distribution which demonstrates the potential that this technique has for providing detailed chemical information with high spatial resolution.

6 REFERENCES

1. J. Israelachvili, *Intermolecular and Surface Forces*, 2nd ed, Academic Press, London, 1992.
2. G. Binnig, C.F. Quate, and C. Gerber, *Phys. Rev. Lett.*, **56**, 930-933 (1986).
3. G. Binnig, H. Rohrer, Ch. Gerber, and E. Weibel, *Phys. Rev. Lett.*, **49**, 57-62 (1982).
4. C.M. Knobler and D.K. Schwartz, *Curr Opin Coll Inter Sci*, 4 (1), 46-51 (1999).

5. A. Ulman, *Chem. Rev.*, **96** (4), 1533-1554 (1996).
6. J. Caspers, E. Goormaghtigh, J. Ferreira, R. Brasseur, M. Vandenbranden and J-M. Ruysschaert,, *J. Colloid Interface Sci.*, **91**, 546-553 (1983).
7. C.P. Smith, and H.S. White, *Langmuir*, 9, 1-6 (1993).
8. D.R. Lide, *CRC Handbook of Chemistry and Physics*, 72nd ed, Boca Raton, FL, 1991.
9. J. Zhang, J. Kirkham, C. Robinson, M.L. Wallwork, D.A. Smith, A. Marsh and M. Wong, *Anal. Chem.*, **72**, 1973-1978 (2000).
10. D.A. Smith, M.L. Wallwork, J. Zhang, J. Kirkham, C. Robinson, A. Marsh and M. Wong, *J. Phys. Chem. B*, **104**, 8862-8870 (2000).
11. M.L. Wallwork, D.A. Smith, J. Zhang, J. Kirkham and C. Robinson, *Langmuir*, in press.
12. K.L. Johnson, K. Kendall and A.D. Roberts, *Proc. R. Soc. Lond. A*, **324**, 301-313 (1971).
13. D.V. Vezenov, A. Noy, L.F. Rozsnyai and C.M. Lieber, *J. Am. Chem. Soc.*, **119**, 2006-2015 (1997).
14. S.R. Holmes-Farley, C.D. Bain and G.M. Whitesides, *Langmuir*, **4**, 921 (1998).
15. R.M. Crooks, L. Sun, C. Xu, S.L. Hill and A. Ricco, *J. Spectroscopy*, **8**, 28-33 (1993).
16. E.W. van der Vegte and G. Hadziioannou, *Langmuir*, **13**, 4357-4368 (1997).
17. D. Hadzi, *Theoretical Treatments of Hydrogen Bonding*, Wiley; Chichester, 1997.
18. W.W. Cleland and M.M. Kreevoy, *Science*, **264**, 1887-1890 (1991).
19. J. Chen, M.A. McAllister, J.K. Lee and K.N. Houk, *J. Org. Chem.*, **63**, 4611-4619 (1998).
20. M. Meot-ner and L.W. Sieck, *J. Phys. Chem.*, **90**, 6687-6692 (1986).
21. N. Stahl and W.P. Jencks, *J. Am. Chem. Soc.*, **108**, 4196-4203 (1986).
22. M. Meot-ner, D.E. Elmore and S. Scheiner, *J. Am. Chem. Soc.*, **121**, 7625-7635 (1999).
23. W.J. Bouma and L. Radom, *Chem. Phys. Letts.*, **64**, 216-222 (1979).
24. J. Emsley and R.E. Overill, *Chem. Phys. Letts.*, **65**, 616-623 (1979).
25. S.K. Sinniah, A.B. Steel, C.J. Miller and J.E. Rett-Robey, *J. Am. Chem. Soc.*, **118**, 8925-8931 (1996).
26. K. Koga and X.C. Zeng, *Phys. Rev. Letts.*, 79, 853-858 (1997).

27. J.H. Hoh, J.P. Cleveland, C.B. Prater, J-P Revel, and P.K. Hansma, *J. Am. Chem. Soc.*, **114**, 4917-4922 (1992),
28. S.J. O'Shea, M.E. Welland and T. Rayment, *Appl. Phys. Lett.*, **60**, 2356-2359 (1992).
29. R. Ho, J-Y. Yuan and Z. Shao, *Biophys. J.*, **75**, 1076-1083 (1998).
30. K. Hu and A.J. Bard, *Langmuir*, **13**, 5114-5119 (1997).
31. L.A. Godinez, R. Castro and A.E. Kaifer, *Langmuir*, **12**, 5087-5092 (1996).
32. H.X. He, C.Z. Li, J.Q. Song, T. Mu, L. Wang, H.L. Zhang and Z.F. Liu, *Mol. Cryst. Liq. Cryst.*, **294**, 99-102 (1997).
33. E.W. Van de Vegte and G. Hadziioannou, *J. Phys. Chem. B.*, **101**, 9563-9569 (1997).
34. H.X. He, W. Huang, H. Zhang, Q.G. Li, S.F. Yau Li and Z.F. Liu, *Langmuir*, **16**, 517-521 (2000).
35. D. Leff, L. Brandt and J. Heath, *Langmuir*, **12**, 4723-4730 (1996).
36. L. Liz-Marzan, M. Grersig and P. Mulvaney, *Langmuir*, **12**, 4329-4335 (1996).
37. C. Xu, Li. Sun, L.J. Kepley and R.M. Crookes, *Anal. Chem.*, **65**, 2102-2107 (1993).
38. S.R. Johnson, S.D. Evans and R. Brydson, *Langmuir*, **14**, 6639-6647 (1998).
39. S.D. Evans, S.R. Johnson, Y.L. Cheng and T. Shen, *J. Mater. Chem.*, **10**, 183-187 (2000).
40. J.P. Simmer and A.G. Fincham, *Crit Rev Oral Biol Med*, 6, 82-108 (1995).
41. A.G. Fincham and J. Moradian-Oldak, *Connect Tiss Res*, **32**, 119-124 (1995).
42. J. Zhang, J. Kirkham, M.L. Wallwork, D.A.M. Smith, S.J. Brookes, R.C. Shore, S.R. Wood and C. Robinson, *Langmuir*, **15**, 8178-8183 (1999).
43. J. Kirkham, S.J. Brookes, R.C. Shore, W.A. Bonass, D.A.M. Smith, M.L. Wallwork and C. Robinson, *Connect Tiss Res*, **38**, 91-100 (1998).
44. J. Kirkham, S.J. Brookes, J. Zhang, S.R. Wood, R.C. Shore, D.A.M. Smith, M.L. Wallwork and C. Robinson, *Caries Res*, in press.